APPLICATIONS OF
MODELLING AND SIMULATION
http://arqiipubl.com/ams eISSN 2600-8084 VOL 7, 2023, 111-121

DFU Infection and Ischemia Classification: PSO-Optimized Deep Learning Networks

Audrey Huong[1*], Kim Gaik Tay[1], Nur Anida Jumadi[1], Wan Mahani Hafizah Wan Mahmud[1] and Xavier Ngu[2]

[1]Faculty of Electrical and Electronics Engineering, Universiti Tun Hussein Onn Malaysia, Malaysia
[2]Institute for Integrated Engineering, Universiti Tun Hussein Onn Malaysia, Malaysia

[*]Corresponding author: audrey@uthm.edu.my

Submitted 23 July 2023, Revised 23 September 2023, Accepted 27 September 2023, Available online 01 October 2023.

Abstract: The recognition of infection and local perfusion (i.e., ischemic) status of diabetic foot ulcer (DFU) on a regular and timely basis is crucial to promote wound healing and prevent the development of unwanted complications. The conventional DFU assessment method is limited to scheduled clinic visits, impeding close monitoring of foot lesion progression and its chronicity. This paper presents an efficient Particle Swarm Optimization (PSO)-incorporated framework for classifying DFU infection and ischemia conditions using three deep learning models: AlexNet, GoogleNet, and EfficientNet-B0. The optimized system performed well in all evaluation metrics, ranging between 0.82 and 0.92 and near-perfect scores of 0.97 - 1, respectively, indicating the high performance and robustness of the system for the DFU infection and ischemia classification tasks. These results are better than the recent related studies using the same datasets. This system performs competitively with the deeper and heavier Efficient-B5 model, suggesting the efficiency of the proposed strategy without demanding an extensive network exploration process or elaborative feature selection process. The future of this work includes transferring the technology for DFU management using a mobile-based technology platform to improve outpatient care delivery through rapid recognition of DFU infection and their perfusion to optimize limb salvage outcomes.

Keywords: Diabetic foot ulcer; EfficientNet; Infection; Ischemia; PSO.

1. INTRODUCTION

Diabetes is a health problem that has affected 537 million adults worldwide in 2021 [1]. It was reported that an average of USD 996 billion had been spent on health expenditure and management of the disease [2]. Diabetic foot ulcer (DFU) is ulceration at the foot region common in diabetic mellitus (DM) patients. It is a chronic condition due to multiple and complex interrelated pathophysiological factors that cause trauma to the skin at the foot region. Peripheral neuropathy is a problem commonly found in DM patients, wherein high blood sugar levels damage the motor neurons and nerves in the affected extremities. It leads to anatomical deformity and skin ulcers, reducing pain sensation in the affected skin. The patients are less likely to be receptive to inflicted wounds, leading to delayed treatment-related complications. This is further aggravated by peripheral arterial disease (PAD) in DM patients, where endothelial cells of the blood vessels have been destroyed; this microcirculation dysfunction increases the risk of ulceration and infection. The local hypoxic ischemic environment inhibits wound healing activity and promotes anaerobic bacterial growth [3]. The prevalence of wound infection is largely influenced by the compromised immunology of this patient group. Bacterial infections at the local level may spread to deeper tissues, including joints and bones (known as osteomyelitis), if not promptly identified and managed [4]. This soft tissue infection can also rapidly spread to the circulation, causing sepsis, and foot amputation is necessary to prevent complications.

The primary source of DFU infection is either fungi or bacteria, or both [5]. In contrast, the ischemic wound is due to vascular dysfunction in mixed micro- and macro-levels, impairing the perfusion of local tissues. This chronic and progressive disease can be divided into four categories: (1) nonischemic and noninfected, (2) infection and nonischemic, (3) ischemic and noninfected, and (4) ischemic and infected wounds. The ischemic infected wounds are the most unfavorable and can be fatal if treatment is delayed. Experienced experts would be able to recognize the presence of infection and ischemia in DFU through visual information and physical examination in the primary care settings using the Wagner grading system based on the following six criteria [6]: grade 0: no ulcer but high-risk foot, grade I: superficial skin ulcer, grade II: deep ulcer, grade III: Ulcer with bone involvement, grade IV: Localized gangrene, grade V: Extensive gangrene. The wound category beyond grade III requires amputation. The key challenges of this categorization task are the great diversity in the texture and color descriptors of DFU skins and the asymmetric forms of the lesions. Therefore, a tissue biopsy of the suspected infected DFU is performed to confirm the diagnosis through microbiology examination.

Computer vision is an important technology used in industries and real-world applications for object recognition, detection, and data-driven decision-making. This method has been widely used in DFU management to use images to support diagnosis and treatment planning. The recent works used the convolutional deep learning method in their demonstration due to its ability to capture key patterns and important detailed features in an image without explicitly specifying the relationship between the features of each layer and the output. Past studies used pretrained convolutional neural networks (CNNs), such as AlexNet, GoogleNet, ResNet, and VGGNet, and their variants, to detect the presence of wound infection and ischemia using DFU images [7], [8]. Others in [9] proposed a handcrafted deep learning model designed and optimized for DFU infection and ischemia detections. This process relied on experts' prior knowledge and experiences on the best feature representations for the recognition task. Instead of employing features automatically extracted and learned by CNNs, Nora et al. [10] proposed using texture and color extractors to extract high-level features that correspond to the DFU area as inputs to improve the classification performance of CNNs. Due to the limited dataset available in the public domain, efforts have been made to adopt a data augmentation strategy in [7] and generative and discriminative models to generate synthetic images to enrich the training data and increase model generalization. The same workers in [7] also conducted rigorous experiments exploring and comparing the performance of twelve existing CNN models for the DFU infection and ischemia classification task. The other approaches include modifying network architecture and optimizing training hyperparameters for better classification accuracy. Although optimization algorithms, such as the Bayesian algorithm (BA), Genetic algorithm (GA), and Particle Swarm Optimization (PSO), are available for use, the manual process using the grid search method that requires minimal programming effort is most often used for the problem. The process is laborious and easily prone to local minima. The existing works in [7-10] used the manual search method and reported good classification accuracy for the DFU perfusion status, with recognition scores ranging from 0.90-0.99. However, the performance of these classifiers in predicting DFU infection status remained to be further improved. Since the PSO optimization method was shown in [11] to outperform other optimization methods in terms of faster convergence rate and higher search accuracy, this study incorporates this optimization technique to improve the learning capacity of different pretrained CNNs in predicting infection and ischemic conditions based on DFU images, without involving the exhaustive features selection process or extensive modification of network backbone.

The contributions of this study are two-fold as follows: (1) this study is the first to tune training hyperparameters from DFU infection and ischemia datasets automatically, and (2) we demonstrated the effectiveness of the optimization framework that can increase the generalizability of networks achieved by using a small dataset and without needing network structure enhancement. The remainder of this paper is organized as follows. Section 2 discusses the employed dataset and networks and the proposed optimization strategy. Section 3 presents the experimental results and analysis. Section 4 discusses this study's findings and limitations, and Section 5 concludes this study with a summary and recommendations for future practical applications. All simulations and optimization operations discussed in this paper have been carried out using MATLAB R2023a software and run on an NVIDIA Tesla K80 GPU.

2. METHODOLOGY

2.1 DFU Image Datasets and Model Training

This study used the Diabetic Foot Ulcers Grand Challenge (DFUC-21) dataset (Part B) [12] containing 15,760 DFU images collected from Lancashire Teaching Hospital for demonstration of our strategy. This repository contains datasets of DFU problems: infection and ischemia. These images were collected by a podiatrist and a DFU consultant physician at 30-40 cm from the ulcerated foot. They also assigned ground truth labels for these datasets. The infection dataset contains 2,945 images for each positive and negative class, while the ischemia dataset has 4,935 images for each class. The acquired images have varying sizes of 1600 × 3200 and 3648 × 2748, so they were resized to a dimension of 640 × 640 by the owner of these datasets. Examples of these images are shown in Figure 1. Some images are blurry and have low resolution, such as the last image in the top row on the left of Figure 1(a). In the pre-experiment, attempts have been made to improve the image resolution using the Very-Deep-Super-Resolution (VDSR) method; however, no significant difference has been observed in the model inference performance. Therefore, results from the original dataset are reported and presented here.

The images were randomly split into training, validation, and testing datasets following the 0.6/0.2/0.2 splitting ratio. A constant seed number of 1 was used in the randomization process for the reproducibility of the results. These images were resized to the same size of 224 × 224 × 3 prior to training and testing of the pretrained AlexNet, GoogleNet, and Efficient-B0 used in this study for a fair comparison. These models were chosen due to the relatively shallow architecture of the AlexNet and by taking advantage of the GoogleNet that effectively increases the network width using inception module, which is conducive to improve the classification accuracy. The EfficientNet is an effective deep CNN using a scaling approach to scale all dimensions of depth (d^{Φ}), width (ω^{Φ}), and resolution (r^{Φ}) to extract the finest features in an image. Increasing network depth would capture more invariances, higher resolution feature maps increase localization accuracy, while a wider network extracts finer grain patterns. The compound of these scaling processes is shown in Figure 2. The architecture of the employed models is shown in Figure 3. The EfficientNet model was proposed in [13] using Mobile inverted Bottleneck Convolution (MBConv), which consists of a 1×1 expansion convolutional layer, depth-wise convolution layer, Swish activation, Squeeze-excitation (SE) block, a pointwise convolutional layer and a dropout shown in Figure 4 as the baseline model before a constant compound coefficient (Φ) is used to scale the network depth, width and resolution uniformly. The MBConv types used in Figure 3(c) are of different variants depending on the convolutional filter size (i.e., k = 3×3 or 5×5). The EfficientNet-B0 in Figure 3(c) consists of 16 MBConv modules and is 237 layers deep; it is lightweight, shallow and is the baseline model of the

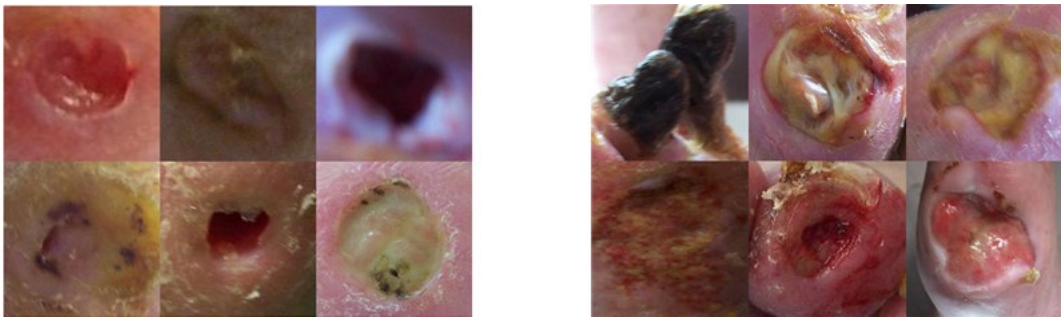

(a) (Left) negative and (right) positive wound infection

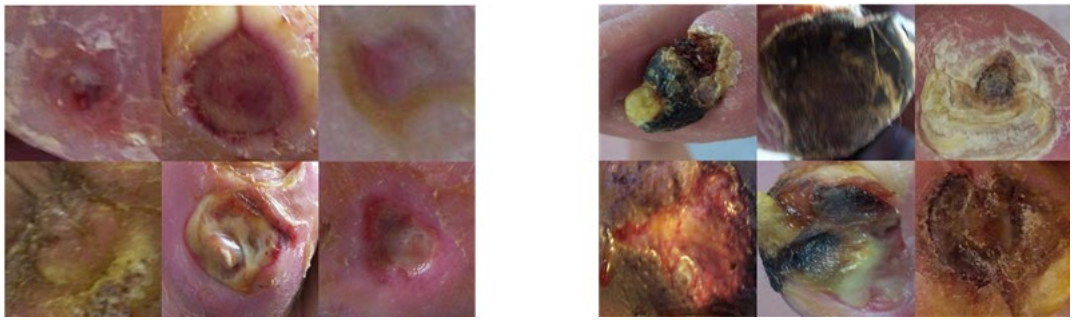

(b) (Left) negative and (right) positive wound ischemia

Figure 1. Example of DFU images with (a) infection and (b) ischemia problems

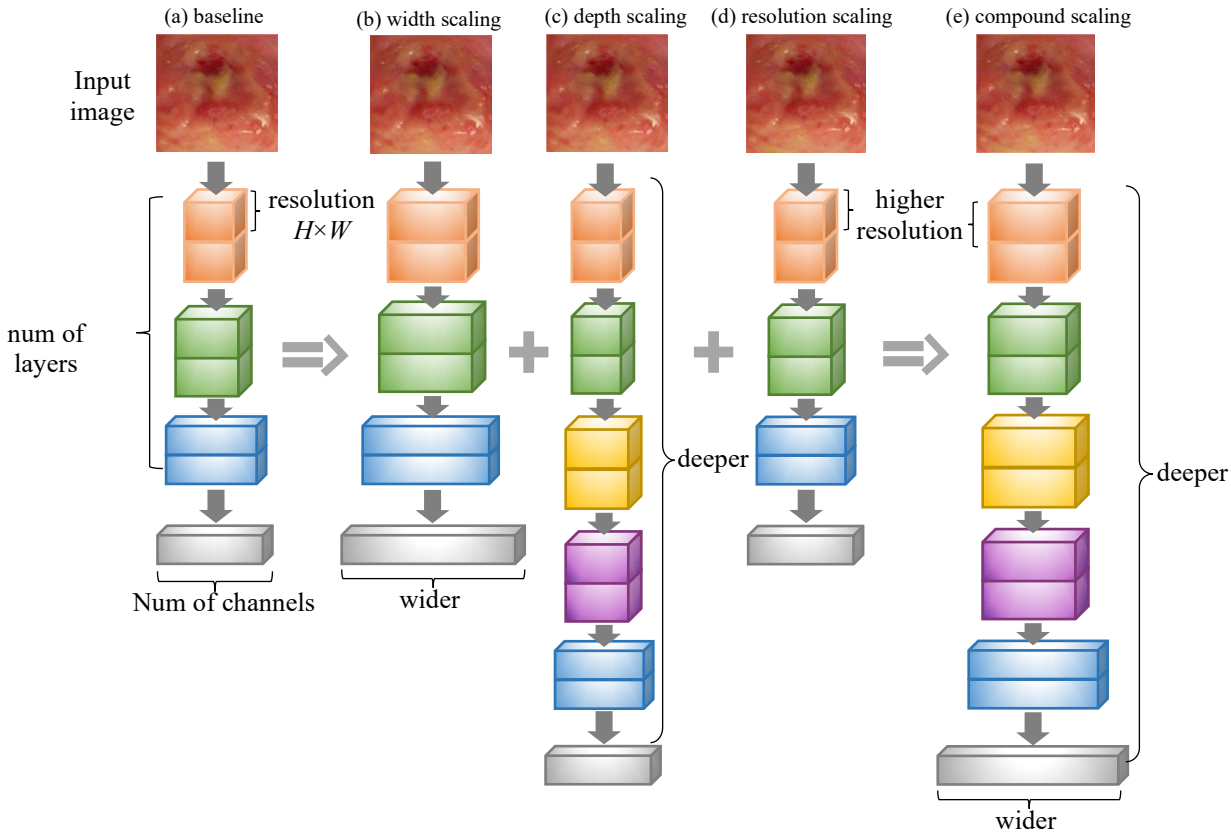

Figure 2. The different single-dimension scaling of a network and compound scaling of EfficientNet. *H*: Height and *W*: width

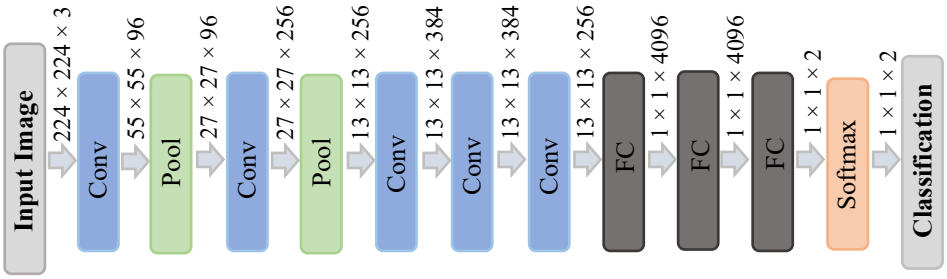

(a)

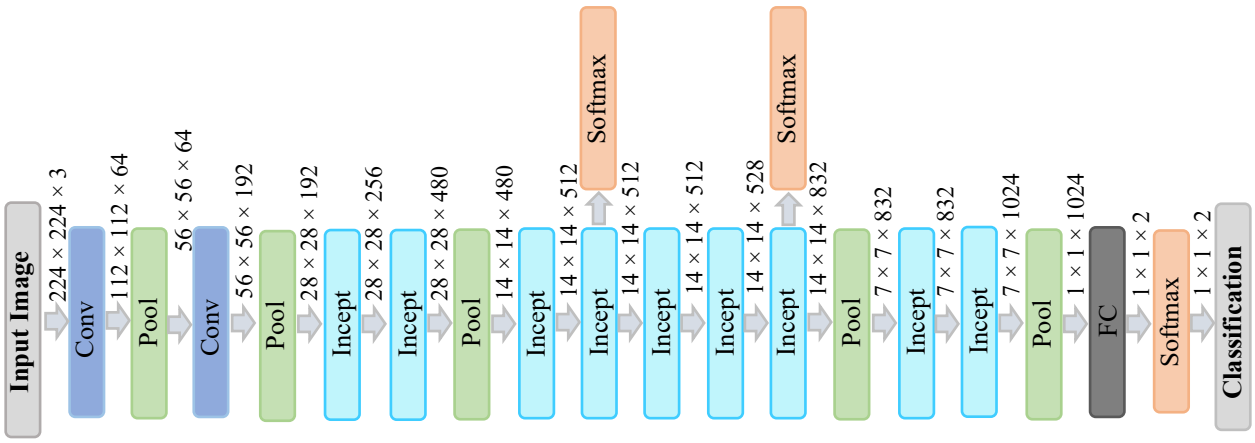

(b)

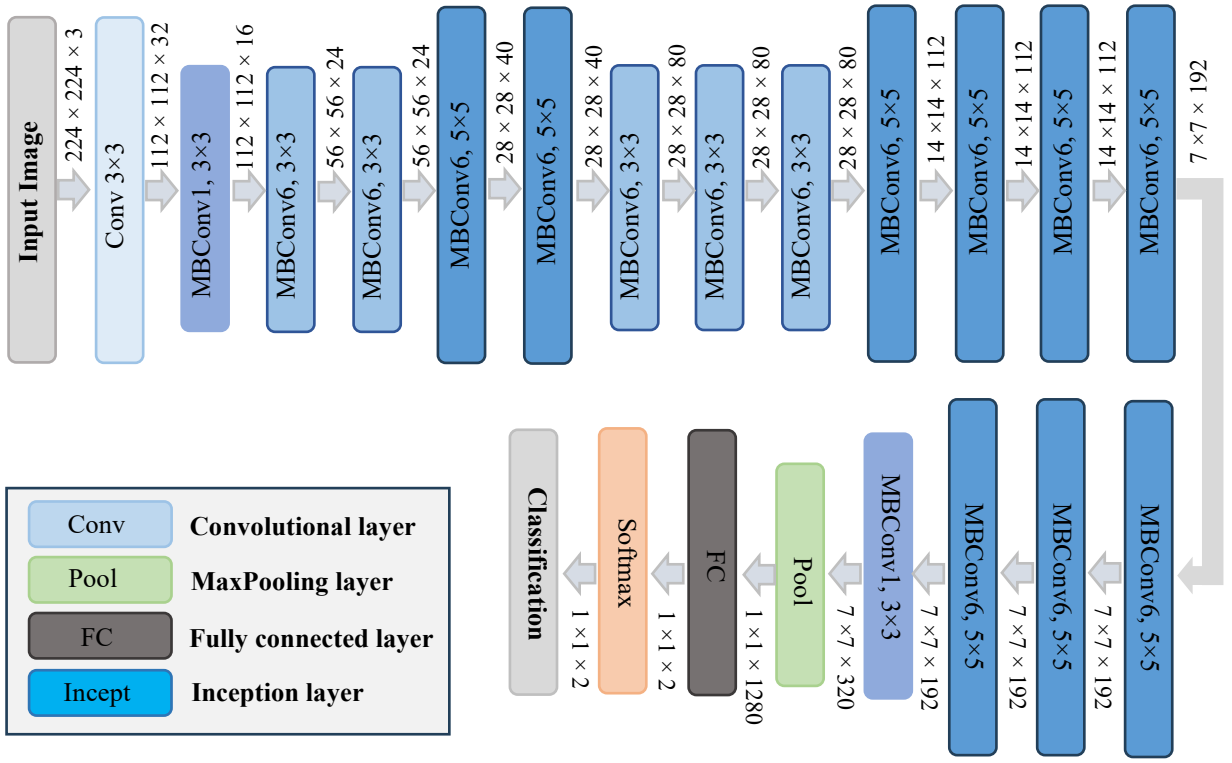

(c)

Figure 3. The network architecture of (a) AlexNet, (b) GoogleNet, and (c) EfficientNet-B0

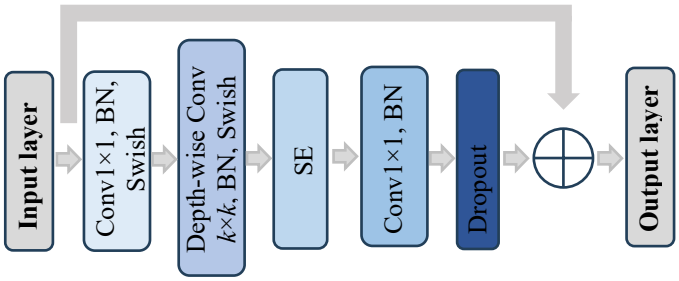

Figure 4. Structure of Mobile inverted Bottleneck Convolution (MBConv). Conv: convolution layer, BN: batch normalization, SE: Squeeze-excitation

Table 1. The upper and lower limits of the considered parameters

Hyperparameter	Lower bound	Upper bound
Solver, L	1 →3: {*Adam*, *Sgdm*, *RMS-Prop*}	
Epoch number, α	50	100
Mini-batch size, β	8	256*/512
Initial learning rate, γ	$1e^{-4}/5e^{-4}$ *	$1e^{-1}$

*EfficientNet-B0 only

scaled versions (i.e., EfficientNet B1-B7) that have an increasing number of MBConv blocks and increasing depth, resolution, width, and model size with the increment in the version. In the case of EfficientNet-B0, the optimal constant value of $d = 1.2$, $\omega = 1.1$, and $r = 1.15$ are determined by grid search when Φ=1 is set and under the constraints: $d \times \omega^2 \times r^2 \approx 2$ [13]. No major modification has been made to the original network architecture, except for the first layer of AlexNet, which has been adjusted to 224 × 224, the same size as the competing networks, and the final three layers of these three models, i.e., Fully connected (FC), Softmax and Classification layer, were modified to two following the binary categorization of wound infection and ischemia (i.e., class labels "0" and "1"). The updated networks are shown in Figure 3. The class label "0" refers to a negative class (noninfection or nonischemic wound), and "1" represents the positive class (i.e., infection or ischemic wound). The networks' backbone was updated during the training to learn features from the images of the infection and ischemia datasets. The validation set estimates the model's performance during training to prevent model overfitting. The network training and optimization framework is shown in Figure 5. To allow an objective demonstration of the optimization method used in the study, we have not considered extensive network modifications, discriminant feature selections, or data enrichment strategies that are well-known as alternative methods to improve classification performance.

2.2 PSO Optimization and Training Hyperparameters

Fine-tuning process of training hyperparameters, such as solver (L), epoch number (α), mini-batch size (β), gradient descent value, and initial learning rate (γ), is often implemented to improve the model's classification accuracy. Unlike most prior studies that used a manual tuning process in the search process, this study used the PSO method. This optimization technique was preferred due to its ability to converge faster and find better solutions than the other methods.

This work fine-tuned four hyperparameters shown in Table 1 to improve the training convergence of the considered networks. This table also shows the search range used for each parameter. A smaller batch size (i.e., limited to 256) and a higher initial learning rate limit (i.e., $5e^{-4}$) are used for EfficientNet-B0 to meet the limitation of the GPU memory. Other factors that influence the selection of these hyperparameter ranges are (1) based on the recommendation of the relevant study [11] for mini-batch size and initial learning rate, (2) the maximum epoch number is empirically decided during the pre-experiment runs, by seeking a balance between computational efficiency and predictive performance. This four-degree optimization process begins with randomly initializing 20 particles in the multidimensional search spaces defined in Table 1. The performance of each particle (i.e., candidate solution) is evaluated in Equation (1). The current best solution, corresponding to the point that produced the least function value in Equation (1), is identified before each particle updates its position and velocity by moving towards that point in the following iteration. The current best solution is updated to the best new solution identified after each iteration. The process was iterated ten times before the global optimal solution was determined at the end of the process.

$$f(T_{acc}, V_{acc}, t) = (100 - T_{acc})^2 + (100 - V_{acc})^2 + {}^{t}/_{1000} \quad (1)$$

T_{acc}, V_{acc}, and t represent training and validation accuracies and training time, respectively. The search is terminated when the validation accuracy fails to increase after ten training iterations or when the maximum epoch number has been reached. This process is repeated for all considered networks before their classification performance is tested using the unseen testing dataset.

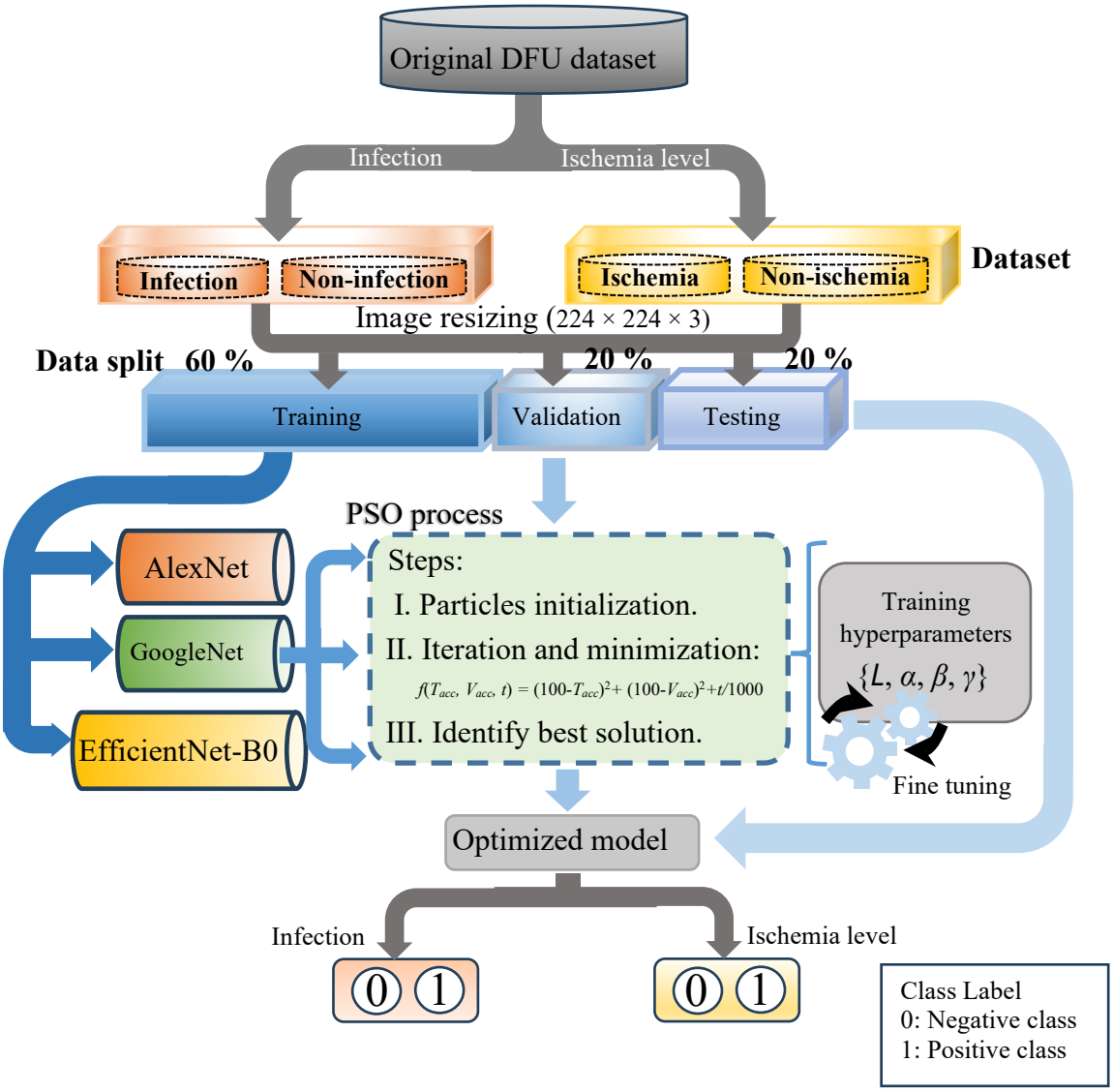

Figure 5. PSO-incorporated DFU infection and ischemia classification framework

Table 2. The best hyperparameters identified for the training of AlexNet, GoogleNet, and EfficientNet-B0 for DFU ischemia and infection classifications

Model	Dataset	Training hyperparameter			
		Solver	Epoch num.	Mini-batch size	Learning rate
AlexNet	Infection	*Adam*	99	512	$1e^{-4}$
	Ischemia	*Adam*	75	512	$1e^{-4}$
GoogleNet	Infection	*Adam*	50	225	$1e^{-4}$
	Ischemia	*Adam*	100	189	$1e^{-4}$
EfficientNet-B0	Infection	*Sgdm*	85	115	0.04
	Ischemia	*Adam*	50	150	$5e^{-4}$

3. RESULTS AND ANALYSIS

The training and optimization framework shown in Figure 5 produced the models optimized for the binary classification of DFU infection and ischemia images. The average search time was recorded as 311 s, 1,250 s, and 1,670 s for AlexNet, GoogleNet, and EfficientNet-B0, respectively, and the best hyperparameters identified for these models from the process are shown in Table 2.

The performance of these optimized networks is evaluated using the testing dataset for infection and ischemia problems shown in Figures 6 and 7, respectively. Figure 8 shows the performance curve of these models and the calculated area under the curve (AUC). Also included on the right of the figure is an inset showing the zoomed-in image of the curves around the

knee point for better visualization. This paper also includes the gradient-weighted class activation map (GradCAM) results for some arbitrarily chosen correctly and incorrectly inferred DFU images in Table 3 for demonstration and discussion. Also shown in the table are the image ground truth (GTruth) label and the predicted (Pred) label.

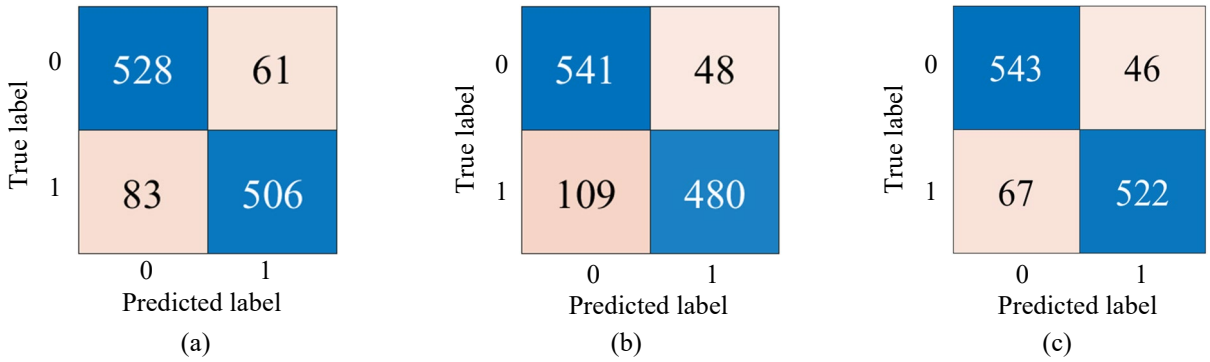

Figure 6. Confusion matrix of (a) AlexNet, (b) GoogleNet, and (c) EfficientNet-B0 optimized for DFU infection classification (class label "0": negative, "1": positive)

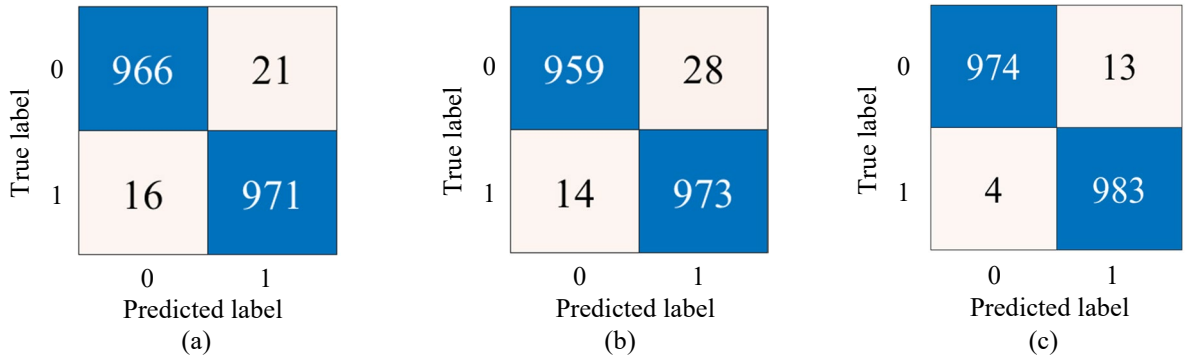

Figure 7. Confusion matrix of (a) AlexNet, (b) GoogleNet, and (c) EfficientNet-B0 for optimized DFU ischemia classification (class label "0": negative, "1": positive)

The results in Figures 6 and 7 are compared using the most common and important performance metrics, namely accuracy (*ACC*), sensitivity (*SENS*), specificity (*SPEC*), and precision (*PREC*), shown in Equations (2)-(5) in Table 4.

a) Accuracy (*ACC*) is the probability of accurate predictions among the total number of predictions.

$$ACC = \frac{TP + TN}{TP + FP + TN + FN} \tag{2}$$

b) Sensitivity (*SENS*) or recall is the rate of correct positive test results among all the predicted true positive outcomes.

$$SENS = \frac{TP}{TP + FN} \tag{3}$$

c) Specificity (*SPEC*) describes the ability of the system to identify negative test results.

$$SPEC = \frac{TN}{TN + FP} \tag{4}$$

d) Precision (*PREC*) is the percentage of the correctly predicted true positive results among all the true positive diagnoses.

$$PREC = \frac{TP}{TP + FP} \tag{5}$$

Table 3. Activation map of AlexNet, GoogleNet, and EfficientNet-B0 overlaid on DFU infection and ischemia images

DFU Image	AlexNet	GoogleNet	EffcientNet-B0
	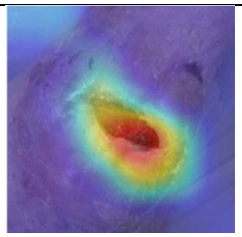	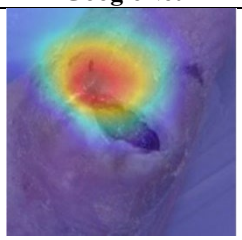	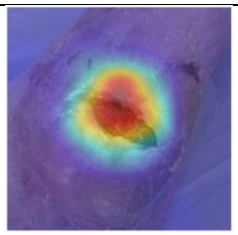
GTruth: Positive infection	Pred: Positive infection	Pred: Positive infection	Pred: Positive infection
(a) Correctly classified positive infection image and models' activation map			
	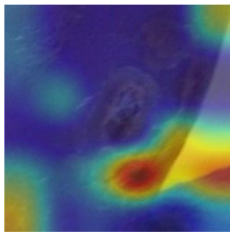	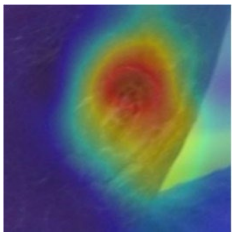	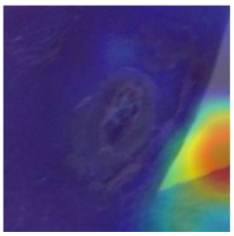
GTruth: Negative infection	Pred: Negative infection	Pred: Positive infection	Pred: Positive infection
(b) Negative infection image misclassified by GoogleNet and EfficientNet-B0 and their activation map			
	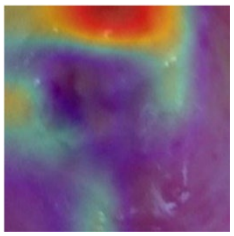	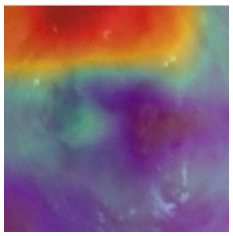	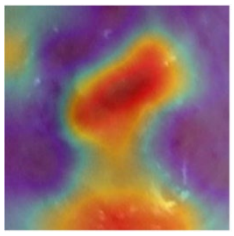
GTruth: Positive ischemia	Pred: Positive ischemia	Pred: Positive ischemia	Pred: Positive ischemia
(c) Correctly classified positive ischemia image and models' activation map			

Table 4. Comparison results of the proposed system and previous research using the same DFU datasets for binary classification of DFU infection and ischemia images

Study	Model	*ACC*	*SENS*	*SPEC*	*PREC*
Infection problem					
Liu et al. [7]	EfficientNet-B5	0.91	0.90	0.93	0.94
Ahsan et al. [8]	ResNet-50	0.84	0.90	0.86	0.83
Goyal et al. [9]	Ensemble CNNs	0.73	0.71	0.74	0.74
Nora et al. [10]	Color (RGB)-texture coded based CNN	0.74	0.75	0.74	0.74
Ours	AlexNet	0.88	0.86	0.90	0.90
	GoogleNet	0.87	0.82	0.92	0.91
	EfficientNet-B0	0.91	0.89	0.92	0.92
Ischemia problem					
Liu et al. [7]	EfficientNet-B5	0.99	1	0.99	0.98
Ahsan et al. [8]	ResNet-50	0.99	0.99	0.99	0.99
Goyal et al. [9]	Ensemble CNNs	0.90	0.89	0.92	0.92
Nora et al. [10]	Color (RGB)-texture coded based CNN	0.99	0.99	0.99	0.99
Ours	AlexNet	0.98	0.98	0.98	0.98
	GoogleNet	0.98	0.99	0.97	0.97
	EfficientNet-B0	0.99	0.996	0.99	0.99

ACC: accuracy, *SENS*: sensitivity, *SPEC*: specificity, *PREC*: precision

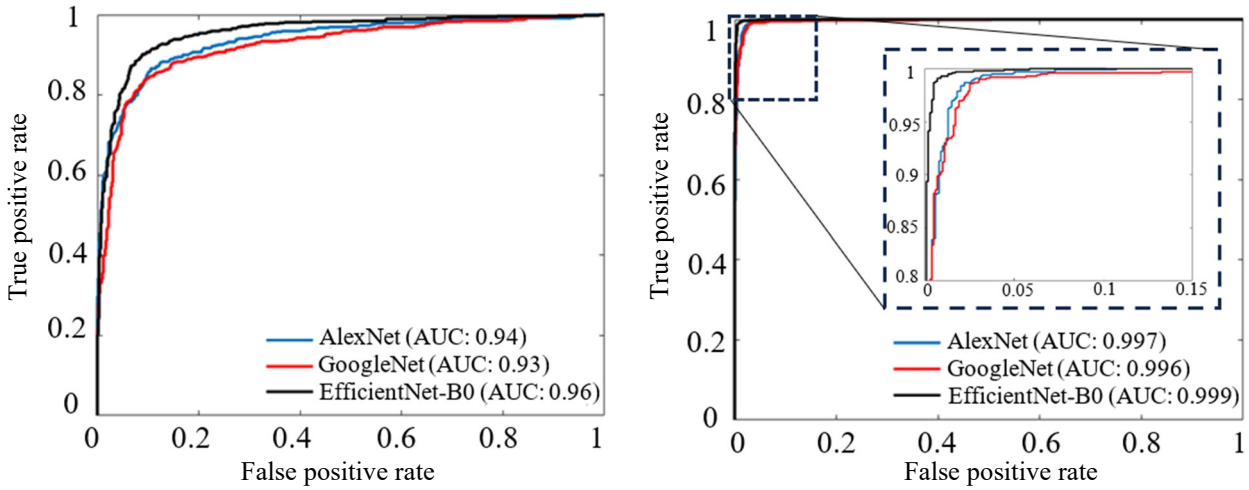

Figure 8. Performance curve of models optimized for DFU infection (left) and ischemia (right) classification problems and the calculated area under the curve (AUC). The figure inset (on the right) is included to better illustrate the curves

TP and *TN* represent the correct classification of the positive and negative samples. *FP* is the misclassification rate of positive samples as negative, while *FN* is the opposite. Also shown in the table are the best results reported in the previous studies in [7-10] using the same dataset for a fair comparison. Studies in [7] employed the same deep learning networks as ours, Goyal et al. [9] designed their networks from scratch, and Nora et al. [10] proposed feature extractors for the same purpose.

4. DISCUSSION

The traditional DFU infection and ischemia classification method is limited to visual inspection during the scheduled clinic visits. This process is time-consuming and prone to high inter and intra-observer variabilities. Misdiagnosis or late or improper treatment often leads to limb amputations to prevent further wound deterioration, causing patients' long-term disability and increasing financial burden. The existing research involved tedious efforts spent meticulously designing a deep model or modifying the existing CNN models to assist clinicians and medical professionals in confirming the diagnosis. This paper addressed these challenges by introducing an optimization strategy in the model training process. The results in Figures 6-8 showed consistently good classification performance of the optimized models. All models demonstrated a higher efficiency in the ischemia foot condition classification than the infection problem. The EfficientNet-B0 produced a superior classification performance for these problems, with a higher average classification accuracy of 0.91 and 0.99 for DFU infection and ischemia classification than the two counterpart models. Despite its better performance, it has many parameters, resulting in a higher average computational time of 5 and 1.3 folds, respectively, compared to AlexNet and GoogleNet. In misclassification, a high false negative rate is usually clinically undesirable because it would result in delayed treatment and recovery. These models performed considerably well in recognizing positive class with good sensitivity results ranging between 0.82 and 0.996, suggesting their potential for practical implementation in real-world settings to detect the presence of DFU infection and ischemia. The remarkably good negative infection detection performance (i.e., high specificity scores of 0.90 – 0.92 in Table 4) shows their ability to avoid unnecessary alarms. Based on Figure 6, AlexNet outperformed GoogleNet for its ability to identify positive infection images better, giving a higher sensitivity of 0.86 in Table 4 and a better discriminative performance with an AUC of 0.94 in Figure 8. EfficientNet-B0 performs best in detecting the positive DFU infection with the highest accuracy and sensitivity metrics of 0.91 and 0.89 and the best AUC of 0.96. The activation maps of these models support this in Table 3(a), which reveals hot (focus) areas crowded around the center of the wound. Since some of the infected DFU areas are covered in the yellow slough, as shown on the top right of Figure 1, EfficientNet-B0 focused on the yellow-colored background scene rather than the target in Table 3(b), causing misclassification. This suggests the need for an instance segmentation model to track and identify wound areas for improved localized classification. Another reason contributing to the misclassification is the poor resolution images that were taken out of focus, such as in Figure 1(a) (top row last image). These images show no distinctive features recognizable by these networks.

Unlike the DFU infection classification problem, this study found that the ischemic status of a DFU image is easier to differentiate by the employed networks. This pattern is consistent with the results reported in the previous studies in Table 4. This is mainly due to significant differences in the morphological, color, and textural features between the ischemic and non-ischemic wounds in Figure 1(b). Most positive ischemic wound images are dominated by hues and shades of greenish-black, which may play an important role in correctly recognizing the class. The networks optimized in this study achieve near-perfect performance in the classification of DFU ischemia status. The results in Table 3(c) proved their remarkable efficiency. Although all models have correctly identified the image as positive ischemia, EfficientNet, which adopts the balanced scaling method, can locate the most relevant features related to the target with great precision for classification.

Among the earlier related research in Table 4, EfficientNet-B5 performed considerably better than other networks. Liu et al. [7] compared the performance of the EfficientNet family in the classification of the DFU datasets, and the computationally heavy EfficientNet-B5 was shown to outperform the smaller variants (B0-B4). This table shows that implementing an automatic optimization strategy like ours produces similarly good results through efficient and effective extraction of useful features for the classification tasks using the smaller and shallower networks. The findings showed that the lighter EfficientNet-B0 (consisting of 237 layers) achieves comparable performance with the deeper B5 model (571 layers long) reported in [7] in all metrics evaluated. These optimized models performed significantly better than the handcrafted approaches demonstrated in references [8] and [9]. This study adopted a strict dataset split of 0.6/0.2/0.2 (training/validation/testing) compared to 0.75/0.15/0.15 in [7], 0.8/0.1/0.1 in [8], and 0.7/0.1/0.2 in [9]. It is hypothesized that the system's performance could be further improved by enlarging the training set or using synthesized images in the training phase.

The search process found differences in the optimal hyperparameters setting identified for each dataset and model in Table 2. In addition to the training and validation accuracies, training time has been included as one of the variables to be minimized in the optimization process. Therefore, the *Adam* optimizer that offers accelerated convergence by adaptively adjusting the learning rate of model parameters is chosen in most experiments as the best solver. The table shows the optimization result of the EfficientNet-B0 trained on the infection dataset, which returns *Sgdm* as the best learner for the generalization task. The *Sgdm* is known to converge slower than the *Adam*; thus, a relatively large learning rate of 0.04 has been chosen to scale the size of the step in the descent direction to accelerate the model training. This search process adopts a random initialization strategy, and these solutions largely depend on the initial point of the search, so this study does not rule out the possibility of convergence to suboptimal solutions. The results also showed that most solutions, especially for initial learning rate and mini-batch size, were stuck at the boundary conditions, a well-known PSO technique limitation [14]. Broader search space coverage has been attempted after the experiments by increasing the boundaries in Table 1, but repeating the process on a larger area with the same number of particles poses a different challenge, as the search process has not sufficiently covered the entire region, leading to an even inferior outcome than the one presented here. Increasing the number of particles and iterations is also not an option due to the complex computational operations exceeding the capacity of our machine. Therefore, other future studies may involve adopting an adaptive optimization algorithm, such as introducing penalty factors to penalize infeasible solutions for a more robust and efficient search for the optimal solution. Infection and ischemia are critical for determining DFU healing, so regular monitoring of these diseases is important to warrant prompt treatment and minimize complications related to the disease. This work may be developed into a practical technology-assisted diagnostic system to assist patient care and improve disease outcomes using a mobile platform.

5. CONCLUSION

Contrary to the traditional approach that dealt with hand-designing a deep network or feature selection methods for DFU infection and ischemia classification, this work adopted an optimization strategy in training the employed pretrained networks for more effective and efficient learning of important features in the dataset. The results showed good classification performance of the optimized models, with the evaluated performance measures ranging from 0.82 to 0.92 and between 0.97 and 1 in detecting DFU infection and ischemia status, respectively. These results are considerably better than the previous studies using the handcrafted network. The proposed system achieved competitive performance compared to the heavier and deeper EfficientNet-B5. This study concluded that the scaling method of EfficientNet allows the model to learn important features more efficiently compared to its shallower counterparts at the price of the higher computational cost. The performance of these classifiers can be further enhanced with data enhancement strategies and a more robust optimization method to prevent premature convergence problems.

FUNDING

This work was partially supported by the Ministry of Higher Education Malaysia through Fundamental Research Grant Scheme (FRGS/1/2020/TK0/UTHM/02/28) and Universiti Tun Hussein Onn Malaysia (TIER1 Q381).

DECLARATION OF CONFLICTING INTERESTS

The authors declare no potential conflicts of interest with respect to the research and publication of this article.

REFERENCES

[1] D. J. Magliano and E. J. Boyko, IDF Diabetes Atlas, *International Diabetes Federation*, 10th ed. Brussels, 2021.
[2] N. Gundluru, D. S. Rajput, K. Lakshmanna, R. Kaluri, M. Shorfuzzaman, M. Uddin and M. A. R. Khan, Enhancement of detection of diabetic retinopathy using Harris Hawks optimization with deep learning model, *Computational Intelligence and Neuroscience*, 2022, 1-13.
[3] A. Stanek, R. Małecki, K. Klimas and A. Kujawa, Different patterns of bacterial species and antibiotic susceptibility in diabetic foot syndrome with and without coexistent ischemia, *Journal of Diabetes Research*, 2021, 1-9.
[4] R. R. Nadia, M. J. Indira, G. O. Ariana, M. M. Yssel, G. N. Gerardo, G. A. David and B. A. Jorge, Wound chronicity, impaired immunity and infection in diabetic patients, *MEDICC Review*, 24, 2022, 44-58.
[5] K. Mponponsuo, R. G. Sibbald and R. Somayaji, A comprehensive review of the pathogenesis, diagnosis, and management of diabetic foot infections, *Advances in Skin & Wound Care*, 34, 2021, 574-581.

[6] Q. Guo, G. Ying, O. Jing, Y. Zhang, Y. Liu, M. Deng and S. Long, Influencing factors for the recurrence of diabetic foot ulcers: A meta-analysis, *International Wound Journal*, 20, 2023, 1762-1775.
[7] Z. Liu, J. John and E. Agu, Diabetic Foot ulcer ischemia and infection classification using Efficientnet deep learning models, *IEEE Open Journal of Engineering in Medicine and Biology*, 3, 2022, 189-201.
[8] M. Ahsan, S. Naz, R. Ahmad, H. Ehsan and A. Sikandar, A deep learning approach for diabetic foot ulcer classification and recognition, *Information*, 14, 36, 2023, 1-10.
[9] M. Goyal, N. D. Reeves, S. Rajbhandari, N. Ahmad, C. Wang and M. H. Yap, Recognition of ischemia and infection in diabetic foot ulcers: Dataset and techniques, *Computers in Biology and Medicine*, 117, 2020, 1-10.
[10] A. G. Nora, R. Ebsim, A. F. H. Alharan and M. H. Yap, Diabetic foot ulcer classification using mapped binary patterns and convolutional neural networks, *Computers in Biology and Medicine*, 140, 2021.
[11] A. Huong, K. G, Tay, K. B. Gan and X. Ngu, A Hierarchical optimisation framework for pigmented lesion diagnosis, *CAAI Transactions on Intelligence Technology*, 1, 2022, 34-45.
[12] M. H. Yap, C. Kendrick, N. D. Reeves, M. Goyal, J. M. Pappachan and B. Cassidy, Development of diabetic foot ulcer datasets: an overview, *Diabetic Foot Ulcers Grand Challenge*, 13183, 2021, 1–18.
[13] M. Tan and Q. V. Le, EfficientNet: Rethinking model scaling for convolutional neural networks, *Proceedings of the 36th International Conference on Machine Learning*, Long Beach, 2019, 6105-6114.
[14] H. L. Minh, S. Khatir, M. A. Wahab and T. C. Le, An enhancing Particle Swarm Optimization Algorithm (EHVPSO) for damage identification in 3D transmission tower, *Engineering Structures*, 241, 2021, 1-23.